Int. J. Heat Mass Transfer. Vol. 35, No. 9, pp. 2077–2085, 1992
Printed in Great Britain

0017-9310/92 $5.00+0.00

Vortex instability of mixed convection flow over horizontal and inclined surfaces in a porous medium

JIIN-YUH JANG and KUN-NUN LIE
Department of Mechanical Engineering, National Cheng-Kung University, Tainan 70101, Taiwan

(*Received* 30 *November* 1991)

Abstract—A linear stability theory is used to analyse the vortex instability of mixed convection boundary layer flow in a saturated porous medium adjacent to an inclined surface where the wall temperature is a power function of the distance from the origin and the external flow is aiding and uniform. In the main flow analysis, both the streamwise and normal components of the buoyancy force are retained in the momentum equations. The present formulation permits the angles of inclination ranging from 0 to close to 90 degrees from the horizontal. In addition, the present study provides new vortex instability results for small angles of inclination ($\phi \leqslant 25^\circ$) and more accurate results for large angles of inclination ($\phi > 25^\circ$) than the previous study by Hsu and Cheng (*ASME J. Heat Transfer* **102,** 544–549 (1980)), where the normal component of the buoyancy force in the main flow was neglected.

1. INTRODUCTION

THERMAL buoyancy force plays a significant role in forced convection heat transfer when the flow velocity is relatively small and the temperature difference between the surface and the free stream is relatively large. Analyses of mixed convection have been performed rather extensively for laminar boundary flows along vertical, inclined, and horizontal flat surfaces immersed in a viscous fluid (see, for example, refs. [1–3], and the references cited therein). The analogous problem of mixed convection in a saturated porous medium has also attracted a number of researchers. This is primarily due to a large number of technical applications, such as storage of radioactive nuclear waste materials, transpiration cooling, separation process in chemical industries, filtration, transport processes in aquifers, ground water pollution, etc.

Cheng [4] developed the similarity solutions for mixed convection flow in a saturated porous medium adjacent to impermeable horizontal surfaces. Similarity solutions have been obtained for the special case where the free stream velocity and wall temperature vary according to the same power function of distance. In a subsequent paper, Hsu and Cheng [5] analysed the vortex mode of instability for a horizontal mixed convection in a porous medium. Minkowycz *et al.* [6] used the local non-similarity method to study the buoyancy effects in the parallel and stagnation forced flows in a porous medium where the similarity solutions are not possible. The influence of surface mass flux on mixed convection over horizontal plates in a saturated porous medium was examined by Lai and Kulacki [7].

Merkin [8] and Joshi and Gebhart [9] studied the mixed convection boundary layer flow in a porous medium adjacent to a vertical, uniform heat flux surface. Unlike the isothermal wall case, a similarity solution does not exist and this problem was solved by using the method of matched asymptotic expansions. For non-Darcy flows, the effects of flow inertia, boundary and thermal dispersion on mixed convection heat transfer over a vertical surface in a porous medium have been studied by Ranganathan and Viskanta [10] and Lai and Kulacki [11].

For an inclined surface, the buoyancy force causing motion has a component in both the tangential and normal directions. This causes a pressure gradient across the boundary layer, leading to a theoretical analysis more complicated than that for a horizontal or a vertical surface. By neglecting the normal component of buoyancy force, Cheng [12] showed that, in the main flow analysis, the mixed convection boundary layer flow over an inclined plate in a saturated porous medium can be approximated by the similarity solution for a vertical plate, with the gravity component parallel to the inclined plate incorporated in the Rayleigh number. Following the same approach, Hsu and Cheng [13] have applied a linear stability analysis to determine the condition of onset of stability for flow over an inclined surface. It is apparent that the instability results in ref. [13] are not valid for the angles of inclination from the horizontal that are small. This is because the normal component of the buoyancy force is responsible for the occurrence of the longitudinal vortices; and this component cannot be neglected when the angles of inclination from the horizontal are small.

The purpose of this paper is to re-examine the main flow and vortex instability of mixed convection boundary layer flow over an inclined plate in a saturated porous medium, for the inclined angles from the horizontal, ϕ, ranging from 0° to close to 90°. The wall temperature is a power function of the distance from the origin. Both the streamwise and normal components of buoyancy force are retained in the momentum equations. This is in contrast to the previous analyses by Cheng [12] and Hsu and Cheng [13], that

NOMENCLATURE

a	spanwise wave number
f	dimensionless base state stream function
F	dimensionless disturbance stream function
g	acceleration due to gravity
i	complex number
k	dimensionless wave number
K	Darcy permeability
m	exponent on wall temperature relation
M	mixed convection parameter
Nu_x	local Nusselt number
p	pressure
Pe	local Peclet number
Ra	Darcy modified local Rayleigh number
t	time
T	temperature
u	Darcy's velocity in x-direction
v	Darcy's velocity in y-direction
w	Darcy's velocity in z-direction
x	coordinate in streamwise direction
y	coordinate normal to bounding surface
z	coordinate in spanwise direction.

Greek symbols

α	equivalent thermal diffusivity
β	coefficient of thermal expansion
η	pseudo-similarity variable
θ	dimensionless base state temperature
Θ	dimensionless disturbance temperature
λ	volumetric heat capacity ratio of the saturated porous medium to that of the fluid
μ	fluid viscosity
ξ	transformed streamwise coordinate, $\sqrt{(Pe)}$
ρ	fluid density
ψ	stream function.

Superscripts

*	critical value
′	differentiation with respect to η.

Subscripts

0	basic undisturbed quantities
1	disturbed quantities
∞	condition at infinity
w	condition at wall.

are generally valid for large values of ϕ. The present resulting equations for the main flow do not admit similarity solutions. They are solved by using a suitable variable transformation and employing an efficient finite difference method similar to that described in Cebeci and Bradshaw [14]. The stability analysis is based on the linear theory. The resulting eigenvalue problem is solved by using a variable step-size sixth-order Runge–Kutta integration scheme incorporated with the Gram–Schmidt orthogonalization procedure [15] to maintain the linear independence of the eigenfunctions.

2. ANALYSIS

2.1. *The main flow*

Consider an inclined impermeable surface at T_w aligned parallel to a uniform free stream with velocity U_∞ and temperature T_∞ as shown in Fig. 1, where x represents the distance along the plate from its leading edge, and y represents the distance normal to the surface. The wall temperature is assumed to be a power function of x, i.e. $T_w = T_\infty + Ax^m$, where A and m are constants. The angle of inclination, ϕ, is measured from the horizontal. The following conventional assumptions simplify the analysis. (1) The physical properties are considered to be constant, except for the density term that is associated with the body force. (2) The convecting fluid and the porous matrix are in local thermodynamic equilibrium. (3) Darcy's law and the Boussinesq approximation are employed.

With these assumptions, the governing equations are given by

$$\frac{\partial u}{\partial x}+\frac{\partial v}{\partial y}=0 \tag{1}$$

$$u=\frac{-K}{\mu}\left(\frac{\partial p}{\partial x}+\rho g\sin\phi\right) \tag{2}$$

$$v=\frac{-K}{\mu}\left(\frac{\partial p}{\partial y}+\rho g\cos\phi\right) \tag{3}$$

$$u\frac{\partial T}{\partial x}+v\frac{\partial T}{\partial y}=\alpha\left(\frac{\partial^2 T}{\partial x^2}+\frac{\partial^2 T}{\partial y^2}\right) \tag{4}$$

$$\rho=\rho_\infty(1-\beta(T-T_\infty)) \tag{5}$$

where K is the permeability of the saturated porous medium; β is the coefficient for thermal expansion; and α represents the equivalent thermal diffusivity. The other symbols are defined in the nomenclature.

The pressure terms appearing in equations (2) and (3) can be eliminated through the cross-differentiation. By applying the boundary layer assumptions ($\partial/\partial x \ll \partial/\partial y$, $v \ll u$) and introducing the stream function ψ, which automatically satisfies equation (1), equations (1)–(5) become

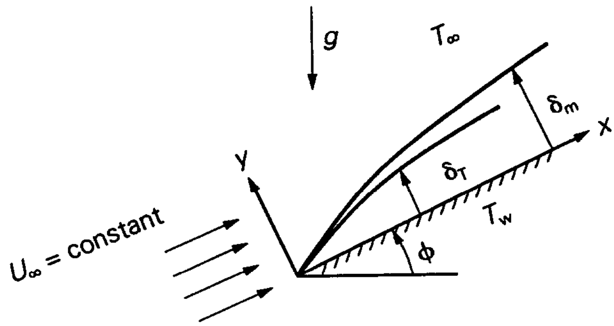

FIG. 1. Physical model.

$$\frac{\partial^2\psi}{\partial y^2} = \frac{\rho_\infty g\beta K}{\mu}\left(\frac{\partial T}{\partial y}\sin\theta - \frac{\partial T}{\partial x}\cos\phi\right) \quad (6)$$

$$\frac{\partial\psi}{\partial y}\frac{\partial T}{\partial x} - \frac{\partial\psi}{\partial x}\frac{\partial T}{\partial y} = \alpha\frac{\partial^2 T}{\partial y^2}. \quad (7)$$

The boundary conditions for this problem are

$$x = 0, \quad y > 0, \quad \frac{\partial\psi}{\partial y} = u_\infty, \quad T = T_\infty$$

$$x > 0, \quad y = 0, \quad \frac{\partial\psi}{\partial x} = 0, \quad T = T_w = T_\infty + Ax^m$$

$$y \to \infty, \quad \frac{\partial\psi}{\partial y} = u_\infty, \quad T = T_\infty. \quad (8)$$

The following dimensionless variables are introduced:

$$\eta(x,y) = \frac{y}{x}Pe^{1/2}$$

$$\xi(x) = Pe^{1/2}$$

$$f(\xi,\eta) = \frac{\psi(x,y)}{\alpha Pe^{1/2}}$$

$$\theta(\xi,\eta) = \frac{T - T_\infty}{T_w - T_\infty} \quad (9)$$

where $Pe = u_\infty x/\alpha$ is the Peclet number.

Then equations (6) and (7) become

$$f'' = M\left[\xi\sin\phi\theta' - \cos\phi\left(m\theta + \frac{\xi}{2}\frac{\partial\theta}{\partial\xi} - \frac{\eta}{2}\theta'\right)\right] \quad (10)$$

$$\theta'' = f'\left(m\theta + \frac{\xi}{2}\frac{\partial\theta}{\partial\xi}\right) - \theta'\left(\frac{1}{2}f + \frac{\xi}{2}\frac{\partial f}{\partial\xi}\right) \quad (11)$$

with boundary conditions

$$f(\xi,0) = 0, \quad \theta(\xi,0) = 1$$

$$f'(\xi,\infty) = 1, \quad \theta(\xi,\infty) = 0 \quad (12)$$

where a prime denotes differentiation with respect to η; and

$$M = \frac{Ra}{Pe^{3/2}}$$

$$Ra = \frac{\rho_\infty g\beta K(T_w - T_\infty)x}{\mu\alpha}$$

is the local Rayleigh number.

It is noted that $M = Ra/Pe^{3/2}$ is the mixed convection parameter, which measures the relative importance of free to forced convection. $M = 0$ corresponds to the case of purely forced convection.

In terms of new variables, it can be shown that the velocity components and the local Nusselt number are given by

$$u = \frac{\partial\psi}{\partial y} = u_\infty f'$$

$$v = -\frac{\partial\psi}{\partial x} = -\frac{\alpha}{2x}Pe^{1/2}\left(f + \xi\frac{\partial f}{\partial\xi} - \eta f'\right)$$

$$Nu_x = -Pe^{1/2}\theta'. \quad (13)$$

2.2. *The disturbance flow*

The standard method of linear stability theory in which the instantaneous values of the velocity, pressure and temperature are perturbed by small amplitude disturbances and the mean flow quantities are subtracted, with terms higher than first order in disturbance quantities being neglected. Then we get the following disturbance equations:

$$\frac{\partial u_1}{\partial x} + \frac{\partial v_1}{\partial y} + \frac{\partial w_1}{\partial z} = 0 \quad (14)$$

$$u_1 = \frac{-K}{\mu}\left(\frac{\partial p_1}{\partial x} - \rho_\infty g\beta\sin\phi T_1\right) \quad (15)$$

$$v_1 = \frac{-K}{\mu}\left(\frac{\partial p_1}{\partial y} - \rho_\infty g\beta\cos\phi T_1\right) \quad (16)$$

$$w_1 = \frac{-K}{\mu}\frac{\partial p_1}{\partial z} \quad (17)$$

$$\lambda\frac{\partial T_1}{\partial t} + u_0\frac{\partial T_1}{\partial x} + v_0\frac{\partial T_1}{\partial y} + u_1\frac{\partial T_0}{\partial x} + v_1\frac{\partial T_0}{\partial y} = \alpha\left(\frac{\partial^2 T_1}{\partial x^2} + \frac{\partial^2 T_1}{\partial y^2} + \frac{\partial^2 T_1}{\partial z^2}\right) \quad (18)$$

where the subscripts 0 and 1 signify the mean flow and disturbance components respectively, and λ is the ratio of the volumetric heat capacity of the saturated porous medium to that of the fluid.

Following the method of order of magnitude analysis described in detail by Hsu and Cheng [5], the terms $\partial u_1/\partial x$ and $\partial^2 T_1/\partial x^2$ in equations (14) and (18) can be neglected. The omission of $\partial u_1/\partial x$ in equation (14) implies the existence of a disturbance stream function ψ_1 such that

$$w_1 = \frac{\partial \psi_1}{\partial y}, \quad v_1 = -\frac{\partial \psi_1}{\partial z}. \tag{19}$$

Eliminating p_1 from equations (15)–(17), and with the aid of equation (19), leads to

$$\frac{\partial u_1}{\partial z} - \frac{\partial^2 \psi_1}{\partial x \partial y} = \frac{\rho_\infty g\beta K}{\mu} \sin\theta \frac{\partial T_1}{\partial z} \tag{20}$$

$$\frac{\partial^2 \psi_1}{\partial y^2} + \frac{\partial^2 \psi_1}{\partial z^2} = -\frac{\rho_\infty g\beta K}{\mu} \cos\theta \frac{\partial T_1}{\partial z} \tag{21}$$

$$\lambda \frac{\partial T_1}{\partial t} + u_0 \frac{\partial T_1}{\partial x} + v_0 \frac{\partial T_1}{\partial y} + u_1 \frac{\partial T_0}{\partial x} - \frac{\partial \psi_1}{\partial z}\frac{\partial T_0}{\partial y} = \alpha\left(\frac{\partial^2 T_1}{\partial y^2} + \frac{\partial^2 T_1}{\partial z^2}\right). \tag{22}$$

As in Hsu and Cheng [5], we assume the three-dimensional disturbances for neutral stability are of the form

$$(\psi_1, u_1, T_1) = [\tilde{\psi}(x,y), \tilde{u}(x,y), \tilde{T}(x,y)] \cdot \exp[iaz] \tag{23}$$

where a is the spanwise periodic wave number. Substituting equation (23) into equations (20)–(22) yields

$$ia\tilde{u} - \frac{\partial^2 \tilde{\psi}}{\partial x \partial y} = \frac{\rho_\infty g\beta K}{\mu} ia \sin\phi \tilde{T} \tag{24}$$

$$\frac{\partial^2 \tilde{\psi}}{\partial y^2} - a^2 \tilde{\psi} = -\frac{\rho_\infty g\beta K}{\mu} ia \cos\phi \tilde{T} \tag{25}$$

$$\alpha\left(\frac{\partial^2 \tilde{T}}{\partial y^2} - a^2 \tilde{T}\right) = u_0 \frac{\partial \tilde{T}}{\partial x} + v_0 \frac{\partial \tilde{T}}{\partial y} + \tilde{u} \frac{\partial T_0}{\partial x} - ia\tilde{\psi}\frac{\partial T_0}{\partial y}. \tag{26}$$

Equations (24)–(26) are solved based on the local similarity approximation [5], wherein the disturbances are assumed to have weak dependence in the streamwise direction (i.e. $\partial/\partial\xi \ll \partial/\partial\eta$).

We let

$$F(\eta) = \frac{\tilde{\psi}(x,y)}{i\alpha Pe^{1/2}}$$

$$G(\eta) = \frac{\tilde{u}(x,y)}{\frac{\alpha}{x} Pe^{1/2}}$$

$$\Theta(\eta) = \frac{\tilde{T}(x,y)}{Ax^m}$$

$$k = \frac{ax}{Pe^{1/2}}. \tag{27}$$

One gets the following system of equations for the local similarity approximations:

$$G = M\xi^2 \sin\phi\Theta - \frac{\eta}{2k} F'' \tag{28}$$

$$F'' - k^2 F = -M\xi k \cos\phi\Theta \tag{29}$$

$$\Theta'' - k^2\Theta = mf'\Theta - \Theta'\left(\frac{1}{2} f + \frac{\xi}{2}\frac{\partial f}{\partial \xi}\right) + \frac{G}{\xi}\left(m\theta + \frac{\xi}{2}\frac{\partial\theta}{\partial\xi} - \frac{\eta}{2}\theta'\right) + k\xi\theta' F. \tag{30}$$

Then the substitution of G and Θ from equations (28) and (29) into equation (30) yields

$$F'''' + \frac{1}{2}\left(f + \xi\frac{\partial f}{\partial\xi}\right)F''' - \left(mf' + 2k^2 + \left(M\xi\sin\phi + \frac{1}{2}\eta M\cos\theta\right)\left(m\theta + \frac{\xi}{2}\frac{\partial\theta}{\partial\xi} - \frac{\eta}{2}\theta'\right)\right)F'' - \frac{1}{2}k^2\left(f + \xi\frac{\partial f}{\partial\xi}\right)F' + k^2\left(mf' + k^2 + M\xi\sin\phi \times\left(m\theta + \frac{\xi}{2}\frac{\partial\theta}{\partial\xi} - \frac{\eta}{2}\theta'\right) + M\xi^2\cos\phi\theta'\right)F = 0 \tag{31}$$

with the boundary conditions

$$F(0) = F''(0) = F(\infty) = F''(\infty) = 0. \tag{32}$$

Equation (31) along with its boundary condition, equation (32), constitutes a fourth-order system of linear ordinary differential equations for the disturbance amplitude distributions $F(\eta)$. For fixed m, M and ϕ, the solution F is an eigenfunction for the eigenvalues ξ and k.

3. NUMERICAL METHOD OF SOLUTION

Equations (10)–(12) for the mean flow were solved by an implicit finite difference scheme similar to, but modified from, that described in ref. [14]. Its details are omitted here. In the stability calculations, the disturbance equations are solved by separately integrating two linearly independent integrals. The full equations may be written as the sum of two linearly independent solutions $F(\eta) = F_1 + cF_2$. The two independent integrals F_1 and F_2 may be chosen so that their asymptotic solutions are

$$F_1 = \exp(-k\eta), \quad F_2 = \exp(-B\eta) \qquad (33)$$

where

$$B = \tfrac{1}{2}(B_1 + \sqrt{(B_1^2 + 4B_2)})$$

$$B_1 = \frac{1}{2}\left(f + \xi \frac{\partial f}{\partial \xi}\right), \quad B_2 = k^2 + m.$$

Equation (31) with boundary condition, equation (32), is then solved as follows. For specified m, M, ϕ, and k, ξ is guessed. Using equations (33) as starting values, the two integrals are integrated separately from the outer edge of the boundary layer to the wall using a sixth-order Runge–Kutta variable size integrating routine incorporated with the Gram–Schmidt orthogonalization procedure [15] to maintain the linear independence of the eigenfunctions. The required input of the base flow to the disturbance equations is calculated, as necessary, by linear interpolation of the stored base flow. From the values of the integrals at the wall, c is determined using the boundary condition $F(0) = 0$. The second boundary condition $F''(0) = 0$ is satisfied only for the appropriate value of the eigenvalue ξ. A Taylor series expansion of the initial guess of ξ provides a correction scheme for the initial guess of ξ. Iterations continue until the second boundary condition is sufficiently close to zero ($< 10^{-6}$, typically).

4. RESULTS AND DISCUSSIONS

Figure 2 shows the effect of the inclination angles ϕ on the dimensionless tangential velocity and temperature profiles across the boundary layer for $m = 0$, $M = 1$, and $\xi = 10$. It is seen that, as would be expected, the dimensionless tangential velocity increases with increasing value of ϕ. It is also seen that, as ϕ increases, the temperature boundary layer thickness decreases and hence the temperature gradient near the wall increases. The dashed lines represent the similarity solutions for an equivalent vertical plate [12], where the normal component of the buoyancy force is neglected in the main flow. It is noted that the equivalent vertical plate solutions have been transformed to present (ξ, η) coordinates for easy comparison with the non-similar solutions. It should be noted that, at $\phi = 0°$, the equivalent vertical plate solutions (dashed lines) are strictly invalid. Note that large calculated differences from the equivalent vertical plate results are apparent for $\phi \leqslant 25°$. That is, the discrepancy is getting larger for small angles of inclination. It is also revealed that the equivalent vertical plate results underestimate the heat transfer rate.

Representative velocity and temperature profiles for $\phi = 0°$ and $\phi = 10°$ are presented in Figs. 3 and 4, respectively, for various values of the buoyancy force parameter M at $m = 0$ and $\xi = 10$. As the buoyancy force parameter M is increased, free convection effects, as expected, are enhanced near the boundary and give rise to greater velocities and temperature gradients near the wall. The local non-similarity solutions of Minkowycz *et al.* [6] for a horizontal plate are also included in Fig. 3. It is shown that our present results are in excellent agreement with those of ref.

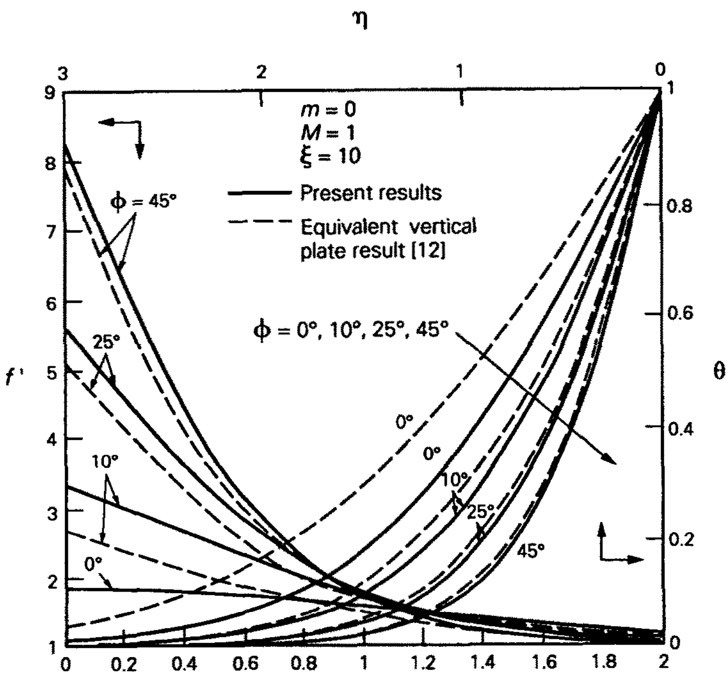

FIG. 2. Tangential velocity and temperature profiles for different angles of inclination for $m = 0$, $M = 1$, $\xi = 10$.

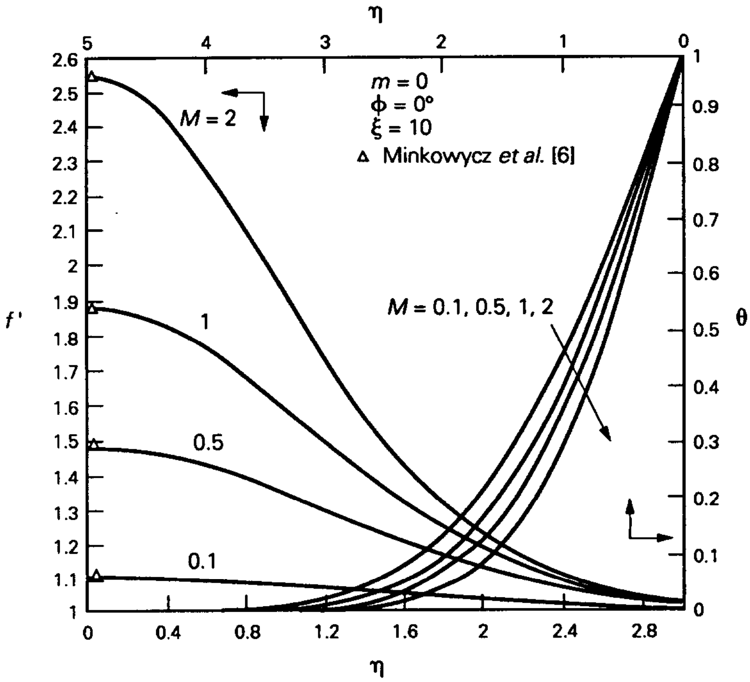

FIG. 3. The tangential velocity and temperature profiles for selected values of M for $\phi = 0°$, $m = 0$, $\xi = 10$.

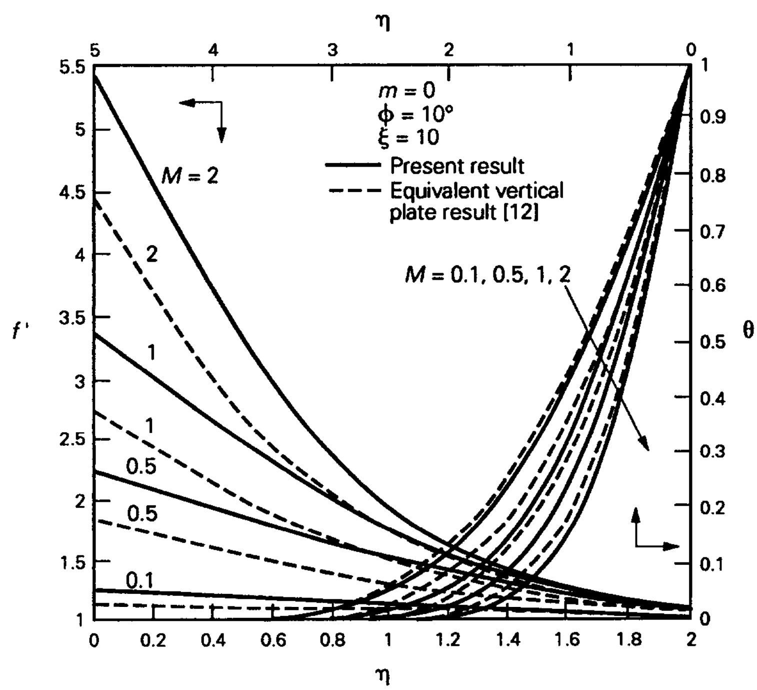

FIG. 4. The tangential velocity and temperature profiles for selected values of M for $\phi = 10°$, $m = 0$, $\xi = 10$.

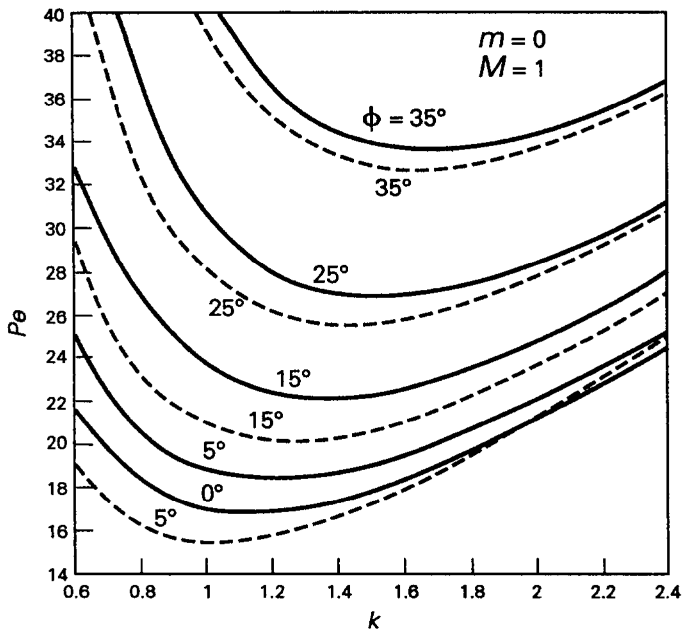

FIG. 5. Neutral stability curves for selected angles of inclination for $m = 0$, $M = 1$. (Dashed lines are presented for equivalent vertical results [13].)

[6]. It is also seen from Fig. 4 that a very large error in transport prediction may arise from the equivalent vertical plate result when the buoyancy force parameter M increases.

Figure 5 shows the neutral stability curves for selected values of ϕ (0°, 5°, 15°, 25° and 35°) at $m = 0$ and $M = 1$. It is seen that as the inclination angle ϕ increases, the neutral stability curves shift to higher Peclet number and higher wave number, indicating a stabilization of the flow to the vortex stability. The dashed lines denote the stability analysis from Hsu and Cheng [13], where the normal component of the buoyancy force was not included in the main flow. It is shown that as ϕ decreases, the two sets of results deviate more. This is due to the fact that for small ϕ the normal component of the buoyancy is not small, so it cannot be neglected.

The critical Peclet numbers as a function of inclination angles for $m = 0$ are plotted in Fig. 6 for various values of buoyancy force parameter M ($M = 0.1$, 0.5, 1 and 5). It can be seen that the flow becomes more susceptible to the vortex instability as the buoyancy force parameter increases. The dashed lines represent the equivalent vertical stability results [13], where the normal component of the buoyancy force was neglected. It is also seen that the equivalent vertical plate assumption leads to significant errors in the stability results as ϕ decreases from 25° down to the horizontal orientation. In addition, as M increases, the deviation in the two sets of results is seen to become larger.

Figure 7 shows the critical Peclet numbers of a horizontal plate ($\phi = 0^\circ$) as a function of the buoyancy force parameter M for different values of the index of power m ($m = -0.5$, 0, 0.5 and 1). For $m = 0.5$ (constant wall heat flux), our present results are in good agreement with those of Hsu and Cheng [5], where the similarity solutions can be obtained. It is observed that the critical Peclet number is a rather strong function of m. The larger the value of m, the more stable the flow for the vortex instability. This is because as m increases, the streamwise temperature increases. Consequently the flow is more stable.

5. CONCLUSIONS

A linear stability analysis is made to re-examine the vortex instability of the mixed convection boundary layer flow over horizontal and inclined surfaces embedded in porous media. Both the streamwise and normal components of the buoyancy force are retained in the momentum equations. Therefore, the present results are valid for the angles in the range of 0° to close to 90° from the horizontal. The results show that the flow becomes less susceptible to vortex mode of disturbances as the buoyancy force is decreased or the plate inclination is increased from the horizontal. It is also found that as the index of power law m increases, the flow becomes less susceptible to the vortex instability. Moreover, the main flow and stability results based on the equivalent vertical plate assumptions are found to be inadequate if the angle of inclination from the horizontal is less than 25°. It should be noted that all the results are based on Darcy's flow model, therefore, they are valid

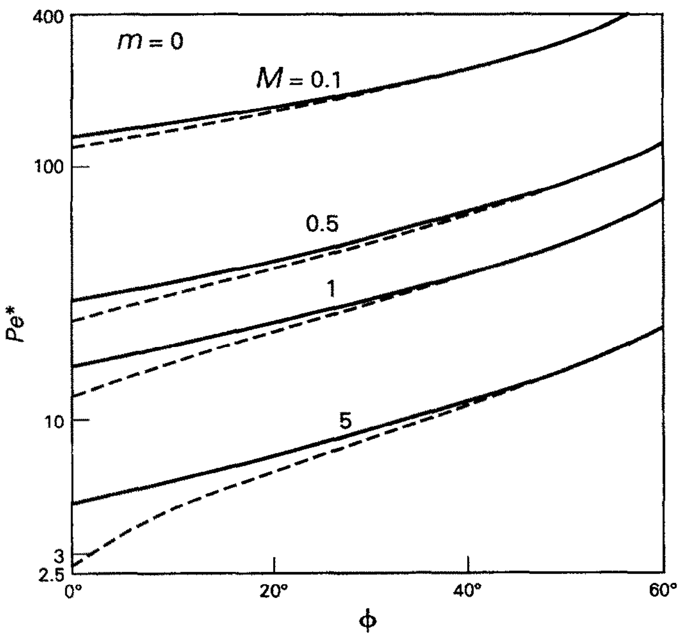

FIG. 6. Critical Peclet numbers as functions of the inclined angle ϕ for selected values of M for $m = 0$. (Dashed lines are presented for equivalent vertical results [13].)

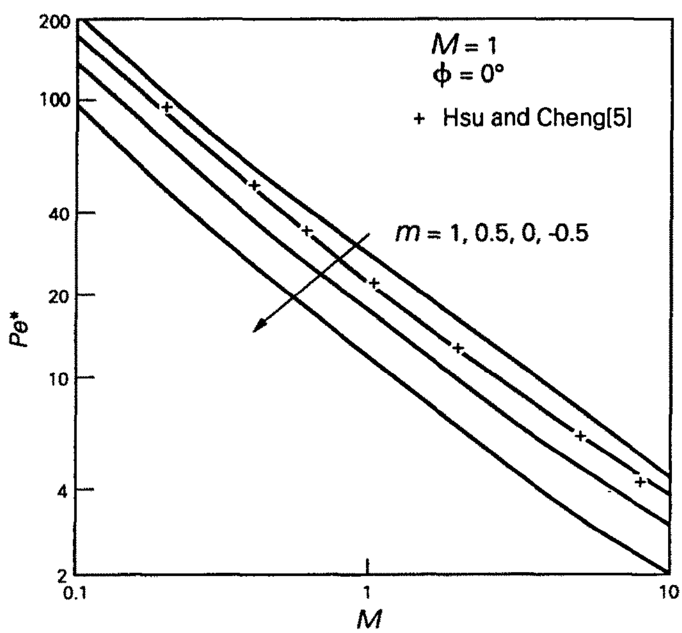

FIG. 7. Critical Peclet numbers as functions of M for selected values of m for $\phi = 0°$, $M = 1$.

strictly for the low-porosity media only. However, in a high porosity medium, there is a departure from Darcy's law and the inertia (velocity-squared term), boundary (no-slip condition) and convective (development term) effects not included in the Darcy law may become significant. This vortex instability problem is currently under investigation by the authors.

REFERENCES

1. T. S. Chen, E. M. Sparrow and A. Mucoglu, Mixed convection in boundary layer flow on a horizontal plate, *ASME J. Heat Transfer* **99**, 60–71 (1977).
2. A. Mucoglu and T. S. Chen, Mixed convection on inclined surfaces, *ASME J. Heat Transfer* **101**, 422–426 (1979).
3. N. Ramachandran, B. F. Armaly and T. S. Chen,

Measurements and predictions of laminar mixed convection flow adjacent to a vertical surface, *ASME J. Heat Transfer* **107**, 637–641 (1985).
4. P. Cheng, Similarity solutions for mixed convection from horizontal impermeable surfaces in saturated porous media, *Int. J. Heat Mass Transfer* **20**, 893–898 (1977).
5. C. T. Hsu and P. Cheng, Vortex instability of mixed convective flow in a semi-infinite porous medium bounded by a horizontal surface, *Int. J. Heat Mass Transfer* **23**, 789–798 (1980).
6. W. J. Minkowycz, P. Cheng and R. N. Hirschberg, Nonsimilar boundary layer analysis of mixed convection about a horizontal heated surface in a fluid-saturated porous medium, *Int. Commun. Heat Mass Transfer* **11**, 127–141 (1984).
7. F. C. Lai and F. A. Kulacki, The influence of surface mass flux on mixed convection over a horizontal plate in a saturated porous medium, *Int. J. Heat Mass Transfer* **33**, 576–579 (1990).
8. J. H. Merkin, Mixed convection boundary layer flow on a vertical surface in a saturated porous medium, *J. Engng Math.* **14**, 301–313 (1980).
9. Y. Joshi and B. Gebhart, Mixed convection in porous media adjacent to a vertical uniform heat flux surface, *Int. J. Heat Mass Transfer* **28**, 1783–1786 (1985).
10. P. Ranganathan and R. Viskanta, Mixed convection boundary-layer flow along a vertical surface in a porous medium, *Numer. Heat Transfer* **7**, 305–317 (1984).
11. F. C. Lai and F. A. Kulacki, Effects of flow inertia on mixed convection along a vertical surface in a saturated porous medium, *Proc. 1988 ASME/A.I.Ch.E. National Heat Transfer Conf.*, Vol. 1, pp. 643–652 (1988).
12. P. Cheng, Combined free and forced convection flow about inclined surfaces in porous media, *Int. J. Heat Mass Transfer* **20**, 807–814 (1977).
13. C. T. Hsu and P. Cheng, The onset of longitudinal vortices in mixed convective flow over an inclined surface in a porous medium, *ASME J. Heat Transfer* **102**, 544–549 (1980).
14. T. Cebeci and P. Bradshaw, *Momentum Transfer in Boundary Layers*, Ch. 7. Hemisphere, Washington, DC (1977).
15. A. R. Wazzan, T. T. Okamura and A. M. O. Smith, Stability of laminar boundary layers at separation, *Physics Fluids* **10**(12), 2540–2545 (1967).

INSTABILITE TOURBILLONNAIRE DE LA CONVECTION MIXTE SUR DES SURFACES HORIZONTALES ET INCLINEES DANS UN MILIEU POREUX

Résumé—Une théorie linéaire de stabilité est utilisée pour analyser l'instabilité tourbillonnaire de l'écoulement à couche limite de la convection mixte dans un milieu poreux saturé adjacent à une surface inclinée dont la température de paroi est une fonction puissance de la distance à partir de l'origine, l'écoulement externe étant favorable et uniforme. Dans l'analyse de l'écoulement principal, on considère dans les équations d'impulsion à la fois les composantes normale et longitudinale de la force de flottement. La présente formulation concerne un angle d'inclinaison allant de zéro jusqu'à 90 degrés à partir de l'horizontale. On trouve des résultats nouveaux d'instabilité tourbillonnaire pour les petits angles d'inclinaison ($\phi \leqslant 25^\circ$) et des résultats pour les grands angles ($\phi > 25^\circ$) plus précis que dans l'étude de Hsu et Cheng (*ASME J. Heat Transfer* **102**, 544–549 (1980)), où la composante normale de la force de flottement a été négligée.

WIRBELINSTABILITÄT BEI DER MISCHKONVEKTION AN WAAGERECHTEN UND GENEIGTEN OBERFLÄCHEN IN EINEM PORÖSEN MEDIUM

Zusammenfassung—Mit Hilfe einer linearen Stabilitätstheorie wird die Wirbelinstabilität bei der Grenzschichtströmung unter Mischkonvektion in einem gesättigten porösen Medium analysiert. Dieses poröse Medium grenzt an eine geneigte Oberfläche, wobei die Wandtemperatur sich gemäß einer Potenzfunktion mit dem Abstand von der Anströmkante ändert. Die äußere Strömung ist mit der Auftriebsströmung gleichgerichtet und gleichmäßig. Die Impulsgleichungen für die Hauptströmung enthalten zwei Komponenten für die Auftriebskraft, eine in Strömungsrichtung und eine senkrecht dazu. Die vorliegende Formulierung erlaubt Neigungswinkel bezüglich der Waagerechten zwischen 0° und näherungsweise 90°. Darüberhinaus werden neue Ergebnisse für die Wirbelinstabilität bei kleinen Neigungswinkeln ($\phi \leqslant 25^\circ$) vorgelegt und für große Neigungswinkel ($\phi > 25^\circ$) genauere Ergebnisse, als sie in einer früheren Untersuchung von Hsu und Cheng (*ASME J. Heat Transfer* **102**, 544–549 (1980), enthalten sind, wo die Normalkomponente der Auftriebskraft vernachlässigt worden war.

ВИХРЕВАЯ НЕУСТОЙЧИВОСТЬ ТЕЧЕНИЯ ПРИ СМЕШАННОЙ КОНВЕКЦИИ НАД ГОРИЗОНТАЛЬНОЙ И НАКЛОННОЙ ПОВЕРХНОСТЯМИ, ПОМЕЩЕННЫМИ В ПОРИСТУЮ СРЕДУ

Аннотация—Линейная теория устойчивости используется для анализа вихревой неустойчивости при смешанной конвекции в пограничном слое в насыщенной пористой среде, прилегающей к наклонной поверхности, причем температура стенки является степенной функцией расстояния, а внешнее течение – спутным и однородным. При анализе основного течения в уравнении сохранения количества движения учитываются составляющие подъемной силы, направленные по потоку и по нормали к нему. В предложенной формулировке допускается изменение углов наклона от 0 до почти 90° от горизонтали. Приводятся новые результаты для вихревой неустойчивости при малых углах наклона ($\phi \leq 25^\circ$), а также более точные результаты для больших углов ($\phi > 25^\circ$), чем полученные в предыдущем исследовании Хсу и Ченга (*ASME J. Heat Transfer* **102**, 544–549 (1980)), где нормальная составляющая подъемной силы в основном течении не учитывалась.